Silver Nanostructures for Fluorescence Correlation Spectroscopy: Reduced Volumes and Increased Signal Intensities

ARTICLE *in* JOURNAL OF PHYSICAL CHEMISTRY LETTERS · SEPTEMBER 2012

Impact Factor: 7.46 · DOI: 10.1021/jz301229m

THE JOURNAL OF PHYSICAL CHEMISTRY Letters

Letter

pubs.acs.org/JPCL

Silver Nanostructures for Fluorescence Correlation Spectroscopy: Reduced Volumes and Increased Signal Intensities

Sharmistha Dutta Choudhury,[†] Krishanu Ray, and Joseph R. Lakowicz*

Center for Fluorescence Spectroscopy, Department of Biochemistry and Molecular Biology, University of Maryland School of Medicine, 725 West Lombard Street, Baltimore, Maryland 21201, United States

Supporting Information

ABSTRACT: Fluorescence correlation spectroscopy (FCS) is a widely used technique to investigate the interactions and dynamics of molecules, below micromolar concentrations. Silver nanostructure (AgNS) substrates can extend the applicability of FCS to higher concentrations, which is useful for many biologically relevant reactions. Additionally, these substrates can improve detection efficiency by increasing fluorescence signal intensities. The ease of preparation of the AgNS substrates in comparison to previously investigated materials prepared by top-down nanofabrication is expected to make them readily available and suitable for various FCS applications.

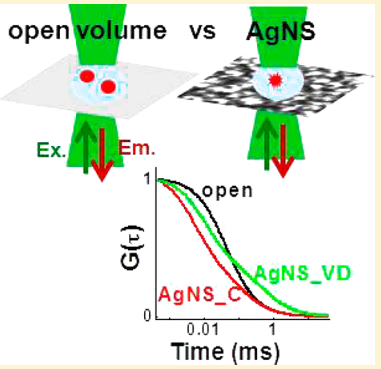

SECTION: Physical Processes in Nanomaterials and Nanostructures

In recent years, we have witnessed a revolution in fluorescence microscopy with the development of technologies that bypass the classical diffraction limit. Introduction of plasmonic structures and advances in super-resolution technologies are opening up new possibilities for the investigation of biological systems in their native, unperturbed state, with high resolution.[1−4] Obtaining subdiffraction fluorescence observation volumes is also fundamental to the improvement of sensitive bioanalytical techniques such as fluorescence correlation spectroscopy (FCS). FCS is widely used to study the interactions and dynamics of molecules based on the fluorescence intensity fluctuations in a small detection volume.[5−7] With typical diffraction-limited observation volumes of about 1 fL obtained with conventional confocal microscopy systems, FCS measurements can only be performed at low fluorophore concentrations (pico- to nanomolar). This severely compromises the ability of FCS to study biological interactions that take place at high concentrations (micro- to millimolar range) or to investigate processes in cellular environments. However, such systems can be investigated with ultralow detection volumes. For example, by reducing the detection volume to ∼1 zL, it can be possible to isolate and observe a single molecule even at a concentration of 1.7 mM.[8]

A number of methods are being explored to increase the upper detection limit in FCS measurements. These include total internal reflection,[9] near-field scanning optical microscopy,[10] stimulated emission depletion,[11] nonradiative excitation fluorescence,[12] electromagnetic confinement with dielectric microspheres,[13] surface plasmon coupled emission,[14] and mechanical confinement in microfluidic channels[15] and in subwavelength metallic nanoapertures.[16] Among these, the use of metallic nanoapertures for FCS is particularly appealing because in addition to reduced detection volumes, the plasmonic properties of metal nanostructures also allow for the tuning of the fluorescence behavior of molecules. This leads to a significant increase in the fluorescence intensities and improves the detection efficiency of single molecules.[17−19] Moreover, the introduction of plasmonic nanostructures has the distinct advantage of making FCS studies feasible at high concentrations without any modification of the conventional optical setup.

Since the pioneering study of FCS within subwavelength metallic apertures by Levene et al.,[16] quite a few notable investigations have been carried out in specially prepared nanoapertures of various shapes and sizes.[20−22] These substrates have mainly been fabricated by electron lithographic techniques or focused ion beam milling on aluminum or gold films. Individual gold nanoparticles have also been found to be effective for volume reduction in FCS.[23] In this Letter, we demonstrate that silver nanostructures prepared by simple wet chemical synthesis (AgNS_C) or thermal vapor deposition (AgNS_VD) can be used as efficient substrates for FCS measurements at high concentrations. Over the past several years, we have established that AgNS are good substrates for metal-enhanced fluorescence over an extended wavelength range (∼380−800 nm) for a wide variety of fluorophores.[24−26] In the present study, we show that the fluorescence

Received: August 21, 2012
Accepted: September 20, 2012
Published: September 20, 2012

   dx.doi.org/10.1021/jz301229m | J. Phys. Chem. Lett. 2012, 3, 2915−2919

enhancement effect of the AgNS is an added advantage that significantly improves the FCS measurements with these substrates.

Figure 1 shows the SEM images of the AgNS substrates prepared by the chemical method (AgNS_C) and by thermal

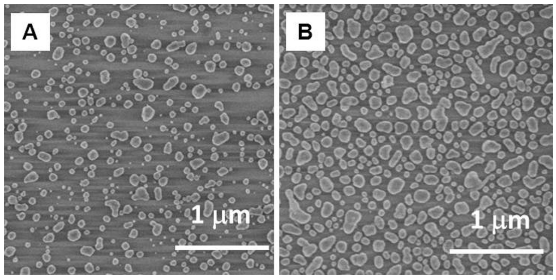

Figure 1. SEM images of (A) AgNS_C and (B) AgNS_VD.

evaporation (AgNS_VD) (see the Supporting Information). The silver nanoparticles are smaller (~60 nm) and more widely spaced (~100−400 nm) on the AgNS_C substrate in comparison to the AgNS_VD (size ≈ 100 nm and spacing ≈ 40−120 nm).

Reflectance images of the same set of AgNS substrates acquired with the confocal microscope system used for FCS measurements are shown in Figure 2. These images are

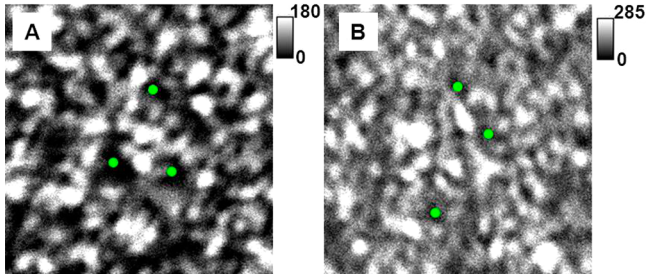

Figure 2. Reflectance images (6 μm × 6 μm) of (A) AgNS_C and (B) AgNS_VD. Scale bars show the respective intensity counts/ms, and the green dots show a few representative dark spots where the excitation laser was focused.

consistent with the SEM images showing a bigger and higher percentage of dark regions, corresponding to the spaces between the nanoparticles, for AgNS_C in comparison to AgNS_VD. As discussed below, the spaces between the nanoparticles act as nanoapertures for confining the detected probe molecules, while, at the same time, the metal nanoparticles create increased near-field excitation profiles. This leads to a reduction in the fluorescence observation volume and allows FCS measurements at high concentrations.

For the FCS studies, first, the different regions on the AgNS substrate were identified from the acquired reflectance image. This was followed by placing a droplet of the aqueous fluorophore (ATTO655) solution on the surface of the substrate and focusing the excitation laser sequentially on several dark spots in the image, using a precisely controlled piezo scanning stage. The ATTO655 was chosen as a suitable probe for the FCS measurements because it does not have any discernible triplet-state dynamics in aqueous solution.[27] The FCS measurements were repeated 10 times in each of the dark spots (corresponding to the nanospaces) of the AgNS substrates. For the reference sample of FCS in open volume, the fluorophore solution was placed on a standard microscope coverslip, and the measurements were carried out under identical experimental conditions. Further details on the experimental setup are provided in the Supporting Information.

Figure 3 shows the intensity−time traces observed due to the diffusion of ATTO655 (50 nM) in the open volume and within

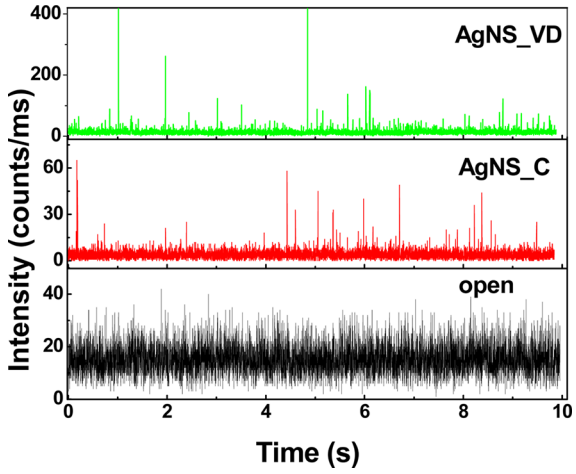

Figure 3. Fluorescence intensity−time traces (1 ms bin) of ATTO655 (50 nM) on a coverslip (open volume), AgNS_C, and AgNS_VD.

the nanospaces on the AgNS. Compared to the open volume, fluorescence bursts with very high signal intensities can be observed on the AgNS. We believe that this interesting behavior is the result of fluorophore−plasmon coupling effects. It is known that the near fields created by the plasmon resonances of metal nanoparticles serve as a source of intense local fields for amplified excitation of vicinal fluorophores. Additionally, excited fluorophores undergo near-field interactions with metallic nanostructures, creating plasmons that then radiate into free space with increased intensities.[24−26] Thus, diffusion of the individual ATTO655 molecules in the proximity of silver nanoparticles can lead to large fluorescence enhancements, as observed in the present case. The higher -intensity fluorescence bursts seen on AgNS_VD in comparison to AgNS_C can be attributed to the larger size of the nanoparticles and smaller intervening spaces in the AgNS_VD substrate, leading to higher metal-enhanced fluorescence.

Further evidence for the fluorophore−plasmon coupling can be obtained by examining the fluorescence intensity decays of the probe on the AgNS. To correlate the fluorescence enhancement with lifetime reduction, the intensity decays on the AgNS substrates have been analyzed by considering only the intense photon bursts (Figure 4). From the fitted curves, the fluorescence lifetime of ATTO655 is found to be ~1.8 ns (open volume), ~0.9 ns (AgNS_C), and ~0.3 ns (AgNS_VD). The significant reduction in the lifetimes on the AgNS surfaces compared to those in the open volume, in conjunction with the observation of intense fluorescence bursts (Figure 3) on the AgNS substrates, suggests that there is an increase in the radiative decay rate of the fluorophore due to the near-field interactions with the metal nanoparticles.[24−26,28] The lifetime reduction is larger (~6-fold) on the AgNS_VD substrate than that on the AgNS_C substrate (~2-fold). This is in accordance with the larger fluorescence signal enhancement on AgNS_VD and the more closely spaced silver nanostructures on this substrate. More insight on the fluorescence enhancement is

dx.doi.org/10.1021/jz301229m | J. Phys. Chem. Lett. 2012, 3, 2915−2919

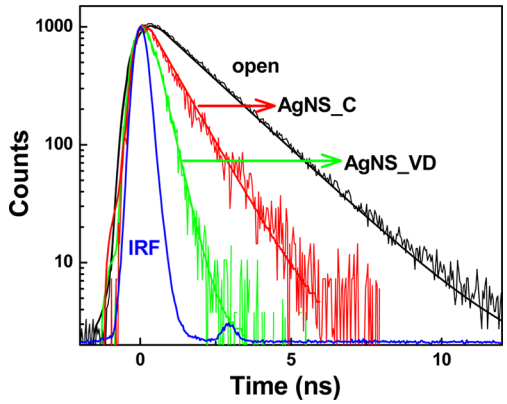

Figure 4. Normalized intensity decays of ATTO655 (50 nM) on a coverslip (open volume), AgNS_C, and AgNS_VD. The intensity decays on the AgNS substrates have been obtained by considering only the intense photon bursts. The solid lines are the fitted curves after reconvolution with the instrument response function, IRF (see the Supporting Information).

obtained by determining the count rates per molecule from the autocorrelation analysis, discussed below.

On the basis of the equilibrium fluctuations of the detected fluorescence intensity, $F(t)$, the autocorrelation function (ACF) is given by

$$G(\tau) = \frac{\langle \delta F(t)\delta F(t+\tau)\rangle}{\langle F\rangle^2} \quad (1)$$

where τ is the delay or lag time and $\langle\ \rangle$ denotes time averaging.[5−7] Figure 5A and B show the characteristic autocorrelations for the fluorescence intensity fluctuations of ATTO655 on the AgNS substrates and in the open volume on a glass coverslip. For a clearer representation, the corresponding data (for 50 nM ATTO655) are normalized and presented in the inset of Figure 5A. Several notable differences, particularly an increase in the amplitude and a decrease in the correlation time (inset, Figure 5A), can be observed for the autocorrelations on AgNS compared to those for the open volume. Interestingly, at 9 μM fluorophore concentration, no time correlation can be observed in the open volume or on AgNS_C, whereas a distinct correlation is observed on AgNS_VD (Figure 5B). These results suggest that there is a reduction in the effective fluorescence detection volume (V_{eff}) on the AgNS substrates, and $V_{eff(AgNS\_VD)} < V_{eff(AgNS\_C)} < V_{eff(open)}$.

For normal Brownian diffusion, in which the mean-square displacement is proportional to time, $\langle \Delta r^2\rangle = 4D\tau$, where D is the diffusion coefficient, the ACF for three-dimensional diffusion of i different diffusing components with relative fractions ρ_i is given by

$$G(\tau) = \frac{1}{N}\sum_i \frac{\rho_i}{(1+\tau/\tau_{d,i})\times\sqrt{(1+\tau/s^2\tau_{d,i})}} \quad (2)$$

Here, $\tau_{d,i} = w^2/4D_i$ are the diffusion times of the particles in the measurement volume, with w being the beam waist and s the ratio between the axial and lateral dimensions of the focal volume. The amplitude of the ACF quantifies the average number of molecules, N, present in the detection volume and also gives an estimate of the fluorescence count rate per molecule, CPM = $(\langle F\rangle - \langle B\rangle)/N$, where $\langle B\rangle$ is the mean background noise.[5−7] From the autocorrelations and the background counts (see the Supporting Information) of several independent measurements at different positions on the AgNS substrates, the average CPM are estimated to be about 3900 cps/molecule in the open volume, ~7500 ± 1500 cps/molecule on AgNS_C, and ~43000 ± 12000 cps/molecule on AgNS_VD. It is clear that the AgNS substrates lead to a considerable increase in the molecular brightness compared to the open volume. The largest enhancement (~11-fold) is observed on the AgNS_VD substrate. Because the reduction in the fluorescence lifetime of ATTO655 on the AgNS_VD is about 6-fold, this means that both the increase in the radiative decay rate as well as the increased excitation intensities in the vicinity of the silver nanostructures are responsible for the enhanced CPM on the AgNS_VD substrates.

The autocorrelation of ATTO655 in the open volume fits well to a single-component three-dimensional diffusion model, with the parameters N = 33, τ_d = 0.051 ms, and s = 5. This is consistent with the known diffusion constant of ATTO655 (400 $\mu m^2 s^{-1}$),[29] and a detection volume of about 1 fL for a diffraction-limited spot in a confocal setup.[5−7] The autocorrelation plots on the AgNS surfaces cannot be fitted to a single-component diffusion model. This is due to the presence of a significant tail in the autocorrelation plots at longer lag times, which is more prominent in the case of AgNS_VD (Figure 5).

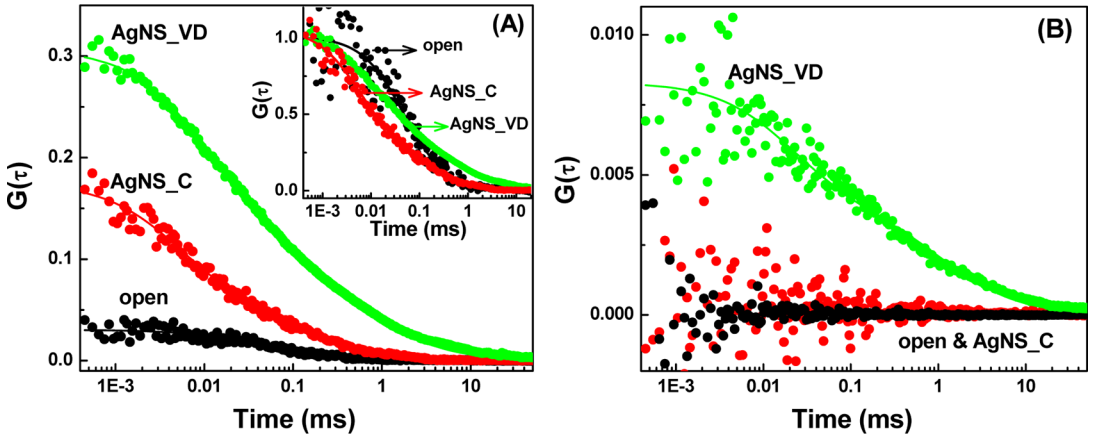

Figure 5. Autocorrelation plots of (A) 50 nM and (B) 9 μM ATTO655 on a coverslip (open volume), AgNS_C, and AgNS_VD. The inset to (A) shows the corresponding normalized autocorrelations.

dx.doi.org/10.1021/jz301229m | J. Phys. Chem. Lett. 2012, 3, 2915−2919

We believe that this tail arises because the silver nanostructures act as obstacles and hinder the normal diffusion of the dyes. Thus, in these cases, the autocorrelations have been fitted to a two-component diffusion model. The average values of the fitted parameters for several measurements at different positions of the substrate are $\tau_{d,1}$ = 0.007 ± 0.005 ms (~70%), $\tau_{d,2}$ = 0.2 ± 0.1 ms (~30%) for AgNS_C and $\tau_{d,1}$ = 0.009 ± 0.004 ms (~70%), $\tau_{d,2}$ = 0.9 ± 0.7 ms (~30%) for AgNS_VD. In these fittings, it is assumed that the ratio between the axial and lateral dimensions of the focal volume on AgNS is the same as that in the open volume, that is, s = 5. This essentially means that the axial and the lateral dimensions of the focal volume are assumed to be modified to the same extent in the presence of the silver nanoparticles. It is also assumed that the two components contributing to the autocorrelation have similar fluorescence brightness.

From a comparison of the diffusion times of ATTO655 in the open volume and on the AgNS surfaces, it is observed that the shorter diffusion time ($\tau_{d,1}$, ~0.007 ms) is about 7-fold less on the AgNS substrates than the normal diffusion time in the open volume (0.051 ms). Because the diffusion coefficient of the dye is unchanged, this decrease in the diffusion time is associated with the reduction in the effective detection volume on the AgNS surfaces compared to that for the open diffraction-limited volume. The diffusion times, $\tau_{d,2}$, on the AgNS substrates are significantly longer than the normal diffusion time in the open volume, and this is attributed to the hindered diffusion or transient caging of the dye molecules in the intervening spaces between the silver nanoparticles. The higher $\tau_{d,2}$ values on AgNS_VD (~0.9 ms) compared to those on AgNS_C ($\tau_{d,2}$ ~0.2 ms) are also consistent with this argument because AgNS_VD has smaller spaces between the silver nanoparticles, and hence, more trapping of the diffusing molecules can be expected (see the Supporting Information).

At higher concentrations of ATTO655 (~9 μM), an effective correlation can only be observed on the AgNS_VD substrate. This indicates that the reduction in the detection volume is most efficient on this substrate. From a statistical analysis of the average amplitudes of the ACF obtained from several independent measurements at different positions on the AgNS substrates, the effective detection volume ($V_{eff} \propto N$) is estimated to be reduced by about a factor of 18 ± 10 on the AgNS_VD substrate and by a factor of 5 ± 2 on the AgNS_C substrate, in comparison to the open volume.

It is worthwhile to mention that molecules that are distant from the AgNS substrate (beyond the near-field coupling distance) also contribute to the observed fluorescence signal. However, these molecules being far away from the plasmonic substrate do not experience any increase in the fluorescence signal intensities. Because the ACF is weighted by the square of the molecular brightness, the contribution from these relatively less fluorescent molecules in the open volume distant from the AgNS is not expected to be significant in the measured autocorrelations.[26] It is also important to note that there is a large variation in the measured diffusion times and the amplitudes of the ACF for the FCS measurements at the different positions on the AgNS surfaces. This reflects the heterogeneity in the various nanospaces on the AgNS substrates (Figures 1 and 2). We anticipate that a controlled, template-guided assembly of the AgNS will lead to the formation of better and more homogeneous surfaces.[30] We are presently exploring this possibility to further improve the performance of the AgNS substrates for FCS.

In summary, we present a simple approach for FCS measurements at micromolar concentrations using AgNS substrates that can be conveniently prepared without any nanofabrication techniques. Despite the fact that these substrates do not have well-defined and isolated compartments, as obtained by nanofabrication, they provide effective reduction of the fluorescence detection volumes by more than an order of magnitude below the diffraction limit. Moreover, the fluorescence enhancement with the present substrates (~11-fold) is quite comparable with that of the structures prepared by nanofabrication. We propose that two effects are responsible for the reduction in the detection volumes in the present substrates. First is the physical confinement of the detected molecules within the nanospaces between the silver nanoparticles, and second is the modification of the near fields in the vicinity of the plasmonic nanoparticles. Because the plasmon-coupled near-field effect exists within a small region (up to ~200 nm) around the metal nanoparticles, this results in the creation of a very small and bright fluorescence volume in the immediate vicinity of these particles. This effect also increases the fluorescence count rates and improves the detectability of single diffusing molecules. The fact that both maximum fluorescence enhancement and the largest reduction in the observation volume are observed on the AgNS_VD substrate gives support to the above proposition.

During the past couple of years, nanophotonics has emerged as a powerful tool for studies with high spatial and temporal resolution. Plasmonic structures have provided new avenues to explore complex dynamic events at the nanoscale, with promising applications in single-molecule DNA sequencing or in characterizing membrane nanodomains. The present study highlights the simplicity with which plasmonic nanostructures can be incorporated on a standard confocal microscopy setup to augment its measurement capabilities. We believe that the plasmonic AgNS substrates will be a widely used platform for performing FCS studies and addressing many biological problems that demand observation volumes below the classical diffraction limit.

■ ASSOCIATED CONTENT

Supporting Information

Figures S1 and S2, fabrication of the AgNS substrates, and experimental setups. This material is available free of charge via the Internet at http://pubs.acs.org.

■ AUTHOR INFORMATION

Corresponding Author

*E-mail: jlakowicz@umaryland.edu.

Notes

The authors declare no competing financial interest.

†Permanent Address: Radiation & Photochemistry Department, Bhabha Atomic Research Center, Mumbai 400085, India.

■ ACKNOWLEDGMENTS

We thank Dr. R. Badugu for many fruitful discussions. This work was supported by NIH Grants HG002655 (J.R.L.) and AI087968 (K.R.). S.D.C. acknowledges the Indo−US Science and Technology Forum (IUSSTF) for the IUSSTF Fellowship.

■ REFERENCES

(1) Genet, C.; Ebbesen, T. W. Light in Tiny Holes. *Nature* **2007**, *445*, 39−46.

(2) Hell, S. W. Toward Fluorescence Nanoscopy. *Nat. Biotechnol.* **2003**, *21*, 1347−1355.
(3) Lezec, H. J.; Degiron, A.; Devaux, E.; Linke, R. A.; Martin-Moreno, L.; Garcia-Vidal, F. J.; Ebbesen, T. W. Beaming Light from a Subwavelength Aperture. *Science* **2002**, *297*, 820−822.
(4) Schermelleh, L.; Heintzmann, R.; Leonhardt, H. A Guide to Super-Resolution Fluorescence Microscopy. *J. Cell Biol.* **2010**, *190*, 165−175.
(5) Haustein, E.; Schwille, P. Fluorescence Correlation Spectroscopy: Novel Variations of an Established Technique. *Annu. Rev. Biophys. Biomol. Struct.* **2007**, *36*, 151−169.
(6) Hess, S. T.; Huang, S.; Heikal, A. A.; Webb, W. W. Biological and Chemical Applications of Fluorescence Correlation Spectroscopy: A Review. *Biochemistry* **2002**, *41*, 697−705.
(7) Schwille, P.; Korlach, J.; Webb, W. W. Fluorescence Correlation Spectroscopy with Single-Molecule Sensitivity on Cell and Model Membranes. *Cytometry* **1999**, *36*, 176−182.
(8) Craighead, H. Future Lab-on-a-Chip Technologies for Interrogating Individual Molecules. *Nature* **2006**, *442*, 387−393.
(9) Hassler, K.; Anhut, T.; Rigler, R.; Gösch, M.; Lasser, T. High Count Rates with Total Internal Reflection Fluorescence Correlation Spectroscopy. *Biophys. J.: Biophys. Lett.* **2004**, L01−L03.
(10) Vobornik, D.; Banks, D. S.; Lu, Z.; Fradin, C.; Taylor, R.; Johnston, L. J. Fluorescence Correlation Spectroscopy with Sub-Diffraction-Limited Resolution Using Near-field Optical Probes. *Appl. Phys. Lett.* **2008**, *93*, 163904/1−163904/3.
(11) Kastrup, L.; Blom, H.; Eggeling, C.; Hell, S. W. Fluorescence Correlation Spectroscopy in Subdiffraction Focal Volumes. *Phys. Rev. Lett.* **2005**, *94*, 178101−178104.
(12) Winckler, P.; Jaffiol, R.; Plain, J.; Royer, P. Nonradiative Excitation Fluorescence: Probing Volumes Down to the Attoliter Range. *J. Phys. Chem. Lett.* **2010**, *1*, 2451−2454.
(13) Gérard, D.; Wenger, J.; Devilez, A.; Gachet, D.; Stout, B.; Bonod, N.; Popov, E.; Rigneault, H. Strong Electromagnetc Confinement Near Dielectric Microspheres to Enhance Single-Molecule Fluorescence. *Opt. Express* **2008**, *16*, 15297−15303.
(14) Calander, N.; Muthu, P.; Gryczynski, Z.; Gryczynski, I.; Borejdo, J. Fluorescence Correlation Spectroscopy in a Reverse Kretchmann Surface Plasmon Assisted Microscope. *Opt. Express* **2008**, *16*, 13381−13390.
(15) Foquet, M.; Korlach, J.; Zipfel, W. R.; Webb, W. W.; Craighead, H. G. Focal Volume Confinement by Submicrometer Sized Fluidic Channels. *Anal. Chem.* **2004**, *76*, 1618−1626.
(16) Levene, M. J.; Korlach, J.; Turner, S. W.; Foquet, M.; Craighead, H. G.; Webb, W. W. Zero-Mode Waveguides for Single-Molecule Analysis at High Concentrations. *Science* **2003**, *299*, 682−686.
(17) Rigneault, H.; Capoulade, J.; Dintinger, J.; Wenger, J.; Bonod, N.; Popov, E.; Ebbesen, T.; Lenne, P.-F. Enhancement of Single-Molecule Fluorescence Detection in Subwavelength Apertures. *Phys. Rev. Lett.* **2005**, *95*, 117401.
(18) Aouani, H.; Wenger, J.; Gérard, D.; Rigneault, H.; Devaux, E.; Ebbesen, T. W.; Mahdavi, F.; Xu, T.; Blair, S. Crucial Role of the Adhesion Layer on the Plasmonic Fluorescence Enhancement. *ACS Nano* **2009**, *3*, 2043−2048.
(19) Wenger, J.; Gérard, D.; Aouani, H.; Rigneault, H. Nanoaperture-Enhanced Signal-to-Noise Ratio in Fluorescence Correlation Spectroscopy. *Anal. Chem.* **2009**, *81*, 834−839.
(20) Lu, G.; Li, W.; Zhang, T.; Yue, S.; Liu, J.; Hou, L.; Li, Z.; Gong, Q. Plasmonic-Enhanced Molecular Fluorescence within Isolated Bowtie Nano-Apertures. *ACS Nano* **2012**, *6*, 1438−1448.
(21) Wenger, J.; Lenne, P.-F.; Popov, E.; Rigneault, H. Single Molecule Fluorescence in Rectangular Nano-apertures. *Opt. Express* **2005**, *13*, 7035−7044.
(22) Blom, H.; Kastrup, L.; Eggeling, C. Fluorescence Fluctuation Spectroscopy in Reduced Detection Volumes. *Curr. Pharm. Biotechnol.* **2006**, *7*, 51−66.
(23) Estrada, L. C.; Aramendía, P. F.; Martínez, O. E. 10000 Times Volume Reduction for Fluorescence Correlation Spectroscopy Using Nanoantennas. *Opt. Express* **2008**, *16*, 20597−20602.
(24) Lakowicz, J. R.; Shena, Y.; D'Auria, S.; Malicka, J.; Fang, J.; Gryczynski, Z.; Gryczynski, I. Radiative Decay Engineering: 2. Effects of Silver Island Films on Fluorescence Intensity, Lifetimes, and Resonance Energy Transfer. *Anal. Biochem.* **2002**, *301*, 261−267.
(25) Lakowicz, J. R.; Ray, K.; Chowdhury, M.; Szmacinski, H.; Fu, Y.; Zhang, J.; Nowaczyk, K. Plasmon-controlled fluorescence: A New Paradigm in Fluorescence Spectroscopy. *Analyst* **2008**, *133*, 1308.
(26) Lakowicz, J. R. *Principles of Fluorescence Spectroscopy*, 3rd ed.; Springer: New York, 2006.
(27) Dertinger, T.; Pacheco, V.; von der Hocht, I.; Hartmann, R.; Gregor, I.; Enderlien, J. Two-Focus Fluorescence Correlation Spectroscopy: A New Tool for Accurate and Absolute Diffusion Measurements. *ChemPhysChem* **2007**, *8*, 433−443.
(28) Wenger, J.; Cluzel, B.; Dintinger, J.; Bonod, N.; Fehrembach, A.-L.; Popov, E.; Lenne, P.-F.; Ebbesen, T. W.; Rigneault, H. Radiative and Nonradiative Photokinetics Alteration Inside a Single Metallic Nanometric Aperture. *J. Phys. Chem. C* **2007**, *111*, 11469−11474.
(29) Müller, C. B.; Loman, A.; Pacheco, V.; Koberling, F.; Willbold, D.; Richtering, W.; Enderlein, J. Precise Measurement of Diffusion by Multi-Color Dual-Focus Fluorescence Correlation Spectroscopy. *Eur. Phys. Lett.* **2008**, *83*, 46001.
(30) Lohmüller, T.; Iverson, L.; Schimdt, M.; Rhodes, C.; Tu, H.-L.; Lin, W.-C.; Groves, J. T. Single Molecule Tracking on Supported Membranes with Arrays of Optical Nanoantennas. *Nano Lett.* **2012**, *12*, 1717−1721.